Geostationary SAR: orbit design and optimization

Matteo Monti [a], Andrea Monti-Guarnieri [a], Naomi Petrushevsky [a], Claudio Prati [a],
Daniela Graziano [b], Alfredo Renga [b], Francesca Pelliccia[b],
Giovanni Paolo Blasone [c], Antonio Montuori [c],
[a] Politecnico di Milano, Piazza Leonardo da Vinci 32, 20133 Milano – It
[b] Università di Napoli "Federico II", 80125 Napoli, It
[c] Agenzia Spaziale Italiana ASI, Via del Politecnico, 00133 Rome

Abstract

Geosynchronous SARs (GEOSAR), studied since the 1970s, are missions providing huge coverage, subcontinental access within minutes, and near continuous observation capabilities. Such missions are suited for imaging and interferometric applications, aiming at large-scale monitoring of deformations, water vapor, and soil moisture. However, maintaining the orbit tube for interferometric requirements is quite demanding due to the perturbing forces at the GEO altitude. Effective control strategies are imperative to keep the baseline and the Doppler band and, ultimately, the orbit shape stable in time. This study investigates the feasibility of the near-zero inclination geostationary SAR concept, considering both interferometric requirements and compliance with the International Telecommunication Union (ITU) Regulation. The orbit maintenance problem is addressed, emphasizing the potential for persistent Earth observation in SAR interferometry applications.

1 Introduction

Forty years ago, the concept of a Synthetic Aperture Radar (SAR) placed in a geosynchronous orbit with a significant orbit plane inclination was first proposed by Kiko Tomiyasu [1]. The concept has received a lot of attention in the literature, and in July 2023, Ludi-Tance 4 01A, the first L-band geosynchronous SAR, was launched by the Chinese Republic. The advantage of such a mission is to imagine large swaths and provide daily revisit and fast access to a wide region. The combination of all-weather, all-time imaging capabilities offered by SAR, with the near-continuous observation potential of a geosynchronous satellite and the huge achievable swaths, make the system unique for monitoring and improving forecasts of fast-evolving phenomena. These include ground motion in landslides, volcanoes, earthquakes, stability of extensive infrastructure, irrigation by soil moisture and water vapor, and inundation [2], [3], [4]. The spread losses due to the long-range, ~37000 km, are partially compensated by a long integration time, in the order of several minutes, and by relatively high transmitted power. A different GEOSAR concept was introduced in [5]: a geostationary near-zero inclination SAR retaining the same advantages of the inclined orbit in terms of the capability to image huge swaths and to achieve sub-daily acquisition revisit. These near-zero inclination systems are much less demanding in power and antenna sizes than the inclined ones, thanks to a much longer integration time (up to some hours). A comparative representation of the two concepts is shown in **Figure 1.1**.

The relative motion condition between the SAR instrument and the observed target zones in the GEO orbit is characterized by very low velocities (Figure 1.1), and this characteristic is paramount for mitigating clutter and Radio Frequency Interference (RFI) [6], [7], [8], [9], [10].

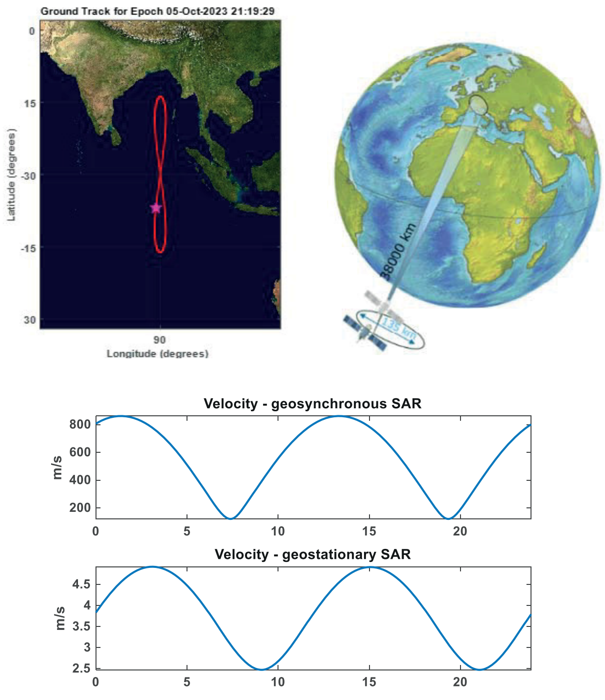

Figure 1.1 Up-left: orbit (ground-track) of Ludi-Tance 4 01A. Up-right: the orbit of a geostationary SAR (scale has been exaggerated for clarity). Bottom: Earth-Centered Earth-Fixed (ECEF) velocities of the two concepts during one orbit period.

For this reason, it is ruled by the International Telecommunication Union (ITU) Regulation, which manages geosta-

ISBN 978-3-8007-6286-6 / ISSN 2197-4403

tionary (GEO) satellite allocation slots in terms of both radio-frequency spectrum and GEO belt occupation [4]. The nearly equatorial orbit provides a North-South line-of-sight, complementary to one of the polar-orbiting SAR-equipped Low Earth Orbit (LEO) satellites and the vast accessible region shown in **Figure 1.2**.

Based on the ITU Recommendations, a geostationary station is asked to maintain its position within a box in longitude limited to ±0.1° for all stations, but the experimental one, for which a larger box of ±0.5° is allowed [4]. For the former case of a ±0.1° box, the relative velocity v is constrained to be < 5 m/s (see **Figure 1.1**). The corresponding Doppler Bandwidth (B) is $2v/L < 1.6$ Hz, assuming a six-meter antenna diameter and the C-band. This contribution is smaller than the one of moving targets from agriculture, B=2-15 Hz in the C-band and from forests in the presence or absence of wind [6], [11], [12]. For all these cases, the longer the integration time, the stronger the attenuation, and the same happens for the RFI.

In addition to ITU Recommendations, the driver for orbit maintenance comes from the interferometric SAR (InSAR) requirements. Diving from the classic East-West and North-South station-keeping logics actuated by the GEO satellites, a geostationary SAR intended for interferometry applications must be more tightly and frequently controlled. The near-zero inclination concept studied here, [5], [13], [14], demands a very accurate orbit stability over the equator, say within 10^{-3} degrees, and the demonstration and quantification of the orbit control feasibility are the primary purposes of this paper.

The paper is organized as follows. Section 2 defines the geostationary SAR concept. Section 3 reviews the main requirements for a SAR mission in C-band that is designed explicitly for interferometric applications and defines the nominal orbit. Section 4 discusses the main perturbations and proposes a strategy for orbit maintenance. The verification of performance against interferometric requirements is outlined in Section 5.

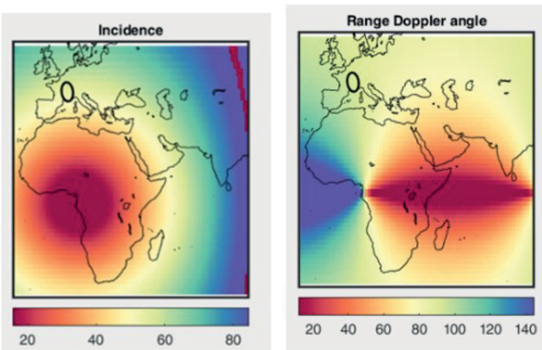

Figure 1.2 Left: incidence angles; Right: Doppler/range angles of a geostationary SAR placed at 10°E of longitude. The best quality is achieved in the yellow areas. The ellipse close to the top-left corner is the beam footprint, of size 400 × 700 km,

2 Geostationary SAR

SAR image acquisitions are enabled by a relative motion between the radar-hosting platform and the observed scene. The ideal point-like ground track of a geostationary satellite is thus not suited for GEOSAR purposes, so perturbations in the eccentricity and/or inclination are needed to enable the synthetic aperture. Therefore, a geosynchronous orbit must be properly defined to meet mission requirements. The non-perturbed orbit in the ECEF reference frame [8] can be approximatively described through the following laws:

$$
\begin{aligned}
r(t) &= R_{geo}\left(1 - e \cdot \cos\left(\Omega_E(t - t_0)\right)\right) \\
\psi(t) &= \psi_0 + 2e \cdot \sin\left(\Omega_E(t - t_0)\right) \\
l(t) &= i \cdot \sin\left(\omega_p + \Omega_E(t - t_0)\right)
\end{aligned} \tag{3.1}
$$

r(t), ψ(t), and l(t) being the polar coordinates (radius, longitude and latitude) of the satellite to the Earth center, t_0 the time of passage at perigee, ψ_0 the central longitude, ω_p the perigee argument, $\Omega_E=2\pi/86164$ rad/s the Earth angular speed and R_{geo}=42164.2 km the orbit semi-major axis. The eccentricity rules the longitudinal displacements of the satellite with respect to its nominal longitude. The inclination determines the satellite's latitudinal motion out of the equatorial plane. Finally, the argument of the perigee establishes the angular shift between both components and the ground-track orientation. The geostationary SAR here designed is conceived to move on an ellipse whose dimensions are determined by eccentricity and inclination. The motion will mainly develop in the longitudinal direction. Thus, the East-West direction of motion will be the direction along which the radar aperture will be synthesized.

The system achieves a wide ground coverage by keeping the antenna beam pointing for a limited time interval, Ts. This will portion the total synthetic aperture that results from (31.):

$$
\mathrm{L}_{max} = \Delta\lambda_{max} \cdot R_{geo} = 4e \cdot R_{geo} \tag{3.2}
$$

into sub-apertures of time extent Ts. The azimuth resolution of a sub-aperture is:

$$
\rho_{az}(\mathrm{t}_0; \Delta t) = \frac{\lambda}{2vT_s} R \simeq \frac{\lambda R}{2R_{geo} \cdot e \cdot \Omega \cos(\Omega t_0) \cdot T_s} \tag{3.3}
$$

where λ is the wavelength, and R is the range. Keeping the integration time Ts constant, the resolution worsens as velocity reduces, being maximum at the perigee (or the apogee), as shown in **Figure 1.1**. The variation of azimuth resolution can be compensated by an inverse variation of the range resolution to keep the imaged area constant. The wanted result is to keep the Signal-to-Noise-Ratio constant for all the sub-apertures.

As can be seen from Equation 3.2 and Equation 3.3, eccentricity rules the GEOSAR performance and, thus, will be a major driver in designing the satellite orbit.

Ideally, any geosynchronous SAR repeats the same orbit every day enabling an interferometric revisit of 24 hours. However, a geostationary SAR could make two interferometric passes in one day by combining acquisitions when the sensor moves east to west with those when it moves in the reverse direction, enabling the interferograms to be sub-daily revisited. If the orbit inclination is null, a zero baseline between subsequent acquisitions can be achieved only at the equator. However, it is possible to tilt the orbit

ISBN 978-3-8007-6286-6 / ISSN 2197-4403

plane by a small inclination angle to get zero baseline at a particular latitude [15]. The sub-daily orthogonal baseline will then progressively increase departing from that latitude, with a rate that depends on the orbit eccentricity. The use of small eccentricity ensures a small sub-daily baseline over a wide interval of latitudes.

3 Mission requirements and Orbit definition

A C-band geostationary SAR characterized by a mean range resolution of 60 m is here conceived to be compliant with ITU Regulation, considering ±0.1° in longitude as the reference box dimensions. The interferometric requirements are driven by the normal baseline and the common Doppler band overlap. In turn, the normal baseline should ensure an elevation of ambiguity, h_a, high enough [16]. If we assume coverage of mid-latitude, then incidence angles higher than 25° (see Fig. 1.2), and we impose $h_a > 100$ m, we get a maximum *orbital tube diameter of 8 km* in C-band. However, the achievement of a sub-daily revisit with that high elevation of ambiguity imposes a further requirement on the incidence angle stability. Finally, the requirement for a common band, say > 70% of the azimuth band of the sub-aperture, in **Figure. 2.1,** results in an additional requirement on the stability of the orbit shape.

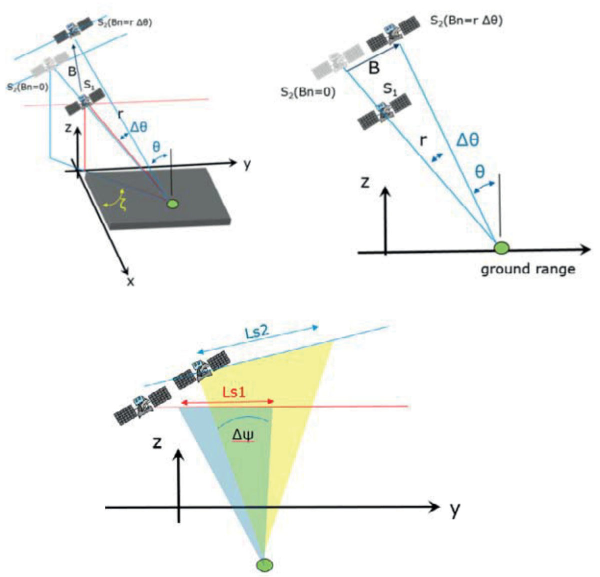

Figure 2.1 Geometry of an interferometric configuration with non-parallel orbits. Up-left: in the 3D plane; Up-right: in the ground range-z plane; Lower plot: exemplification of the common bandwidth concept. The azimuth bandwidth is proportional to the angle Δψ.

These requirements could be very demanding if maintained throughout the whole mission. However, as the major value of a GEO-SAR is in its short-term revisit, an interval of just a few days would be enough to build a significant stack of interferometric images.

The proper definition of the orbit parameters ensures that it meets the assigned requirements. In particular, setting the eccentricity to a value $e = 0.0008$ allows us to achieve the desired imaging capabilities being compliant with the box occupation limits, while a periapsis argument $\omega_p \simeq 90°$ or 270° leads to a symmetric longitudinal track figure enabling specular acquisitions with respect to the vertical axis along the ideal nominal ellipse of motion. The RAAN (Right Ascension of the Ascending Node), Ω_R, is then dimensioned according to the central longitude ψ_0:

$$\Omega_R = t_{sg} + \psi_0 - \omega_p - \theta_a \tag{3.2}$$

where θ_a is the true anomaly and t_{sg} is the Greenwich sidereal time at the orbit periapsis.

In the present design, we assume a central observation in mid-Europe and an epoch consistent with the future EE-12 mission, 15 March 2036 00:00:00 UTCG. The reference orbit parameters can be defined (**Table 3.1)**. A sketch of the nominal orbit is represented on the left in Figure 3.1. The derived satellite ground-track is ellipse-shaped.

a [km]	e	i [deg]	Ω_R [deg]	ω_p [deg]	θ_a [deg]
42165.8	8e-4	0.0051	93.183	90	0

Table 3.1 – GEOSAR nominal orbit parameters.

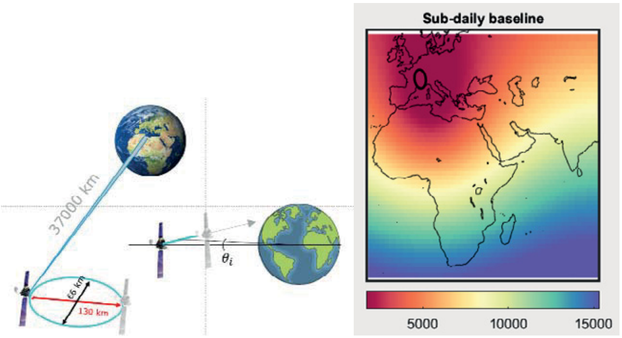

Figure 3.1 Left: geostationary SAR orbit compatible with the ±0.1° assigned box. Center: the tiny inclination of the orbit plane allows for a sub-daily interferometric revisit with zero baseline tuned to a particular latitude. Right: variation of the sub-daily baseline expressed in meters.

As shown in **Figure 3.1** (Center), a tiny inclination angle, $i = 0.0051°$, is assigned to the orbit plane, according to [9], and this value is optimized for targets placed at 41° of latitude. The sub-daily orthogonal baseline will thus be zero for that latitude and will vary between 0 and 15 km over a large portion of the observed zone, as represented in **Figure 3.1** on the right.

4 Orbit maintenance

The orbital tube maintenance is crucial for a geostationary SAR intended for interferometric applications. The GEO communication satellites already in orbit periodically (weekly or monthly) perform East-West and North-South station-keeping maneuvers to counteract the trajectory deviations caused by the perturbing accelerations.

ISBN 978-3-8007-6286-6 / ISSN 2197-4403

At the GEO altitude, the main perturbing accelerations are due to the Earth's non-sphericity, the third-body gravitational attraction (lunar-solar gravitational accelerations), and the solar radiation pressure. For these satellites, the aim is just to maintain the platform in the assigned box. Instead, for a geostationary SAR, the ideal nominal orbit parameters defined in Table 3.1 must be more frequently controlled with acceptable tolerance ranges to ensure the orbit tube's maintenance. Thus, to control a GEOSAR with low eccentricity and low inclination, a cycle of control maneuvers in one sidereal period has to be implemented and applied every certain number of days (from 1 to 7 days) to assure the motion repeatability against the perturbing accelerations that cause the satellite instability in its nominal position.

The maneuvering cycle is implemented as follows:

1. A tangential burn is applied at the perigee to correct the semi-major axis, the mean longitude, and the eccentricity.
2. An out-of-plane burn is applied at the first node to correct the inclination.
3. A tangential burn is applied at the apogee to correct the semi-major axis, the mean longitude, and the eccentricity, and a radial burn is applied to correct the argument of perigee.
4. An out-of-plane burn is applied at the second node to correct the inclination.

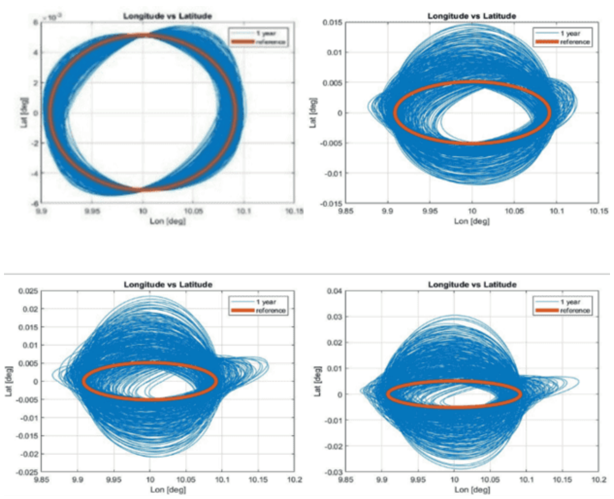

Figure 4.1 Ground-track representation of 365 consecutive orbits obtained by applying the maneuvering cycle every day (Top left), every three days (Top right), every five days (Bottom left), and every seven days (Bottom right).

The goal of each cycle is to correct the effects of the perturbations in order to achieve, after a desired number of days, an orbit with similar orbital characteristics to the previous ones in terms of shape, inclination, and longitudinal position, as it can be seen in **Figure 4.1** in which one-year simulation orbit control results are shown. In the analysis carried out herein, a spherical model with $m/A = 0.025$ kg/m^2 (where m is the satellite mass and A is the area exposed to the Sun) and reflectivity of the satellite $C_R = 1.8$ has been assumed to simulate the solar radiation pressure.

The sum of all the ΔVs needed in one year for each strategy is reported in **Table 4.1**. By reducing the maneuvering frequency, a ΔV saving can be achieved. In particular, the total budget was reduced up to 62% by choosing the 7-day strategy instead of the 1-day strategy. In general, the total maintenance cost is mainly determined by the out-of-plane maneuvers, which are the most expensive ones. Other expensive corrections are the radial burns needed to correct the argument of perigee and keep the ground-track symmetry with respect to the vertical axis. The GEOSAR frozen orbit maintenance involves these corrections that are not typically applied in the classic station-keeping strategies, and this is another critical aspect to address in this novel control strategy concept.

	1 day	3 days	5 days	7 days
ΔV [m/s]	141.09	136.23	114.43	88.52

Table 4.1 ΔV budget per year for each maneuver strategy.

5 Interferometric performance verification

A critical issue in the orbit maintenance strategy definition is the compliance with the requirement of the orbital tube, or – equivalently, the baseline. Imposing that the tube is continuously kept frozen with respect to the fixed reference orbit maneuvering day by day, the maintenance cost will be quite high, and this could potentially limit the duration of the mission, as in [10].

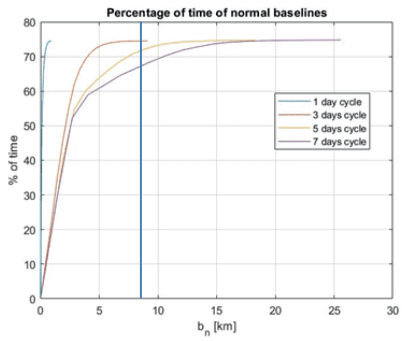

Figure 5.1 Cumulative distribution of the normal baseline in the four different maneuvering strategies for a target at (10°E, 41°N). The vertical line corresponds to the 8 km requirement.

By relaxing the maneuver frequency, significant savings in ΔV can be achieved. However, a proper trade between ΔV and interferometric performance has to be found. In the analysis, one has to discard time intervals of about 3 hours in which sensors is close to the orbit nodes, since in that position the velocity is so small to prevent the formation of the synthetic aperture (see, **Figure 1.1**).

The interferometric performances here reported are evaluated by considering an observed area on ground placed at (10°E, 41°N). **Figure 5.1** and **Table 5.1** report the cumulative distribution of the normal baseline, that's to say the percentage of time in which the baseline is kept within a

ISBN 978-3-8007-6286-6 / ISSN 2197-4403

certain value for different maneuvering strategies. In particular, the values reported within braces in **Table 5.1** have been normalized to the "useful" acquisition time – that is by excluding the passing over the ascending nodes. Notice that the 8 km requirement, which can be assumed as a boundary, is met for about 90% of the 'useful' time for controls up to seven days.

	1 day	3 days	5 days	7 days
$B_n < 4$ km	75% (100%)	70% (93%)	61% (81%)	59% (79%)
$B_n < 5$ km	75% (100%)	73% (97%)	64% (85%)	61% (81%)
$B_n < 8\ km$	75% (100%)	74% (99%)	71% (95%)	67% (89%)
$B_n < 10$ km	75% (100%)	75% (100%)	73% (97%)	69% (92%)

Table 5.1 Time in which the normal baseline values comply with the mission requirements in the four control strategy cases, one year simulation. The values in braces are normalized to the 'useful' time in which the sensor has an effective synthetic aperture.

As for the sub-sidereal baseline, the cumulative probabilities are reported in **Figure 5.2** and in **Table 5.2**. Achieving the required sub-daily baseline requires a very accurate keeping of the orbit inclination (latitude) whose drift is impactful even on the temporal scale of one orbit period. The result is that the 8 km boundary is kept for 90% of the acquisitions if maneuvering is less than 5 days, that is far more demanding than for the daily baseline.

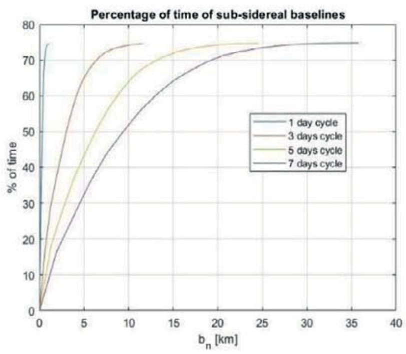

Figure 5.2 Cumulative distribution of the sub-daily normal baseline in the four different maneuvering strategies for a target placed at (10°E, 41°N).

	1 day	3 days	5 days	7 days
$B_n < 4\ km$	75% (100%)	59% (79%)	38% (51%)	27% (36%)
$B_n < 5\ km$	75% (100%)	65% (87%)	43% (57%)	33% (44%)
$B_n < 8\ km$	75% (100%)	73% (97%)	58% (77%)	47% (63%)
$B_n < 10\ km$	75% (100%)	74% (99%)	64% (85%)	52% (69%)

Table 5.2 Time in which the sub-daily normal baseline values are compliant with the mission requirements in the four control strategy cases, 1 year simulation.

Another fundamental issue that has to be addressed is compliance with the common angular (or Doppler) band requirement. In order to correctly perform interferometry, the spectral content between two subsequent acquisitions must be as similar as possible, meaning there has to be a good percentage of overlap between the angular bands spanned by the respective apertures. The nominal band has been considered by taking the total angular band of the reference "frozen" orbit defined in Table 3.1.

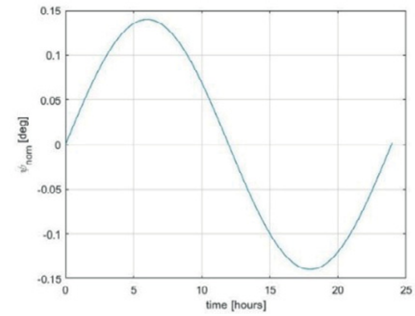

Figure 5.3 Angular band of the reference "frozen" orbit with respect to the nominal position on the ground.

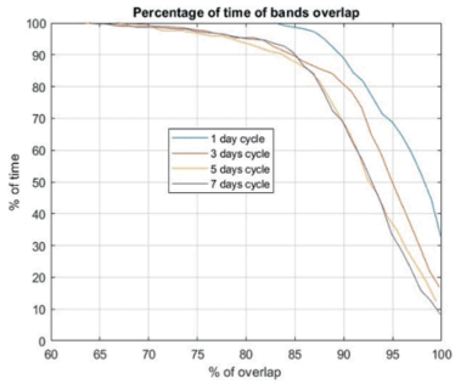

Figure 5.4 Cumulative distribution of common band (percentage of overlap), referred to a target placed at (10°E, 41°N), computed by assuming the four different maneuvering strategies.

The total angular band is $\pm 0.14°$. However, the reference band has to be scaled by 25% to exclude image acquisitions during the passage at the nodes, thus, a reference band of $\pm 0.1225°$ is achieved. **Figure 5.4** plots the cumulative distribution of the percentage of overlap – estimated during one year of propagation – for the four different maneuvering strategies. The same results are reported in **Table 5.3**. One observes that for all the cases, the overlap is above 68%; however, an 80% overlap – that we may assume a very good score, needs maneuvering in less than five days.

	1 day	3 days	5 days	7 days
90% overlap	89%	81%	68%	68%

Table 5.3 Doppler band overlap performances

From these results, it can be observed that very good performance can be achieved by maneuvering every day. In particular, values of the normal baseline under 2 km can be kept for an entire year with a minimum band overlap of approximately 80%. However, the total cost of 141 m/s is

ISBN 978-3-8007-6286-6 / ISSN 2197-4403

quite high. On the other hand, the 7-day maneuvering interval leads to results that are at the limit of acceptable performance, yet with a significant saving in ΔV, which is less than 90 m/s in one year. A 5-day interval could be a good compromise.

6 Conclusion

A Synthetic Aperture Radar placed in a geostationary orbit, compliant with ITU Regulation, takes advantage of a small eccentricity to use long integration times – thus mitigating all the causes affecting the sensitivity, that is, thermal, clutter noise, and Radio Frequency Interferences. The GEOSAR mission is unique for imaging huge swaths at medium resolution, virtually at any time of the day, and achieving an interferometric revisit of 24 hours. Furthermore, a properly dimensioned low inclination orbit allows the system to achieve an interferometric revisit of less than 12 hours. A preliminary analysis of orbit maintenance has been conducted, outlining the definition of a novel control strategy based on the subsequent application of tangential, normal, and radial impulsive burns in one orbit period. It has been shown that a proper control strategy could be the one in which the maneuvering frequency is close to 5 days with a total ΔV of 114.43 m/s per year for a C band mission. This is much more than the usual requirements for a GEO satellite orbit keeping. However, it is still a feasible figure for a GEO-SAR mission. It is worth noting that this is the first result, coming from a very preliminary design, and better performances could be achieved after further studies.

7 Acknowledgments

This work has been supported by the Italian Space Agency in the framework of ASI project "Images", contract n. 2023-32-HH.0, and prof. Mauro Massari of Politecnico di Milano, Dipartimento di Scienze e Tecnologie Aerospaziali, for his valuable input.

8 Literature

[1] K. Tomiyasu and J. L. Pacelli, "Synthetic Aperture Radar Imaging from an Inclined Geosynchronous Orbit," *Geosci. Remote Sens. IEEE Trans. On*, vol. GE-21, no. 3, pp. 324–329, Jul. 1983.

[2] R. Haagmans *et al.*, "Earth Explorer 10 Candidate Mission Hydroterra, ESA Report for Assessment," 2020.

[3] D. Palmisano, A. Balenzano, G. Satalino, F. Mattia, N. Pierdicca, and A. Monti-Guarnieri, "Sentinel-1 sensitivity to soil moisture at high incidence angle and its impact on retrieval," in *International Geoscience and Remote Sensing Symposium (IGARSS)*, 2018, pp. 1430–1433. doi: 10.1109/IGARSS.2018.8518613.

[4] M. Lagasio *et al.*, "A Synergistic use of a high-resolution numerical weather prediction model and high-resolution earth observation products to improve precipitation forecast," *Remote Sens.*, vol. 11, no. 20, 2019, doi: 10.3390/rs11202387.

[5] C. Prati, F. Rocca, D. Giancola, and A. Monti Guarnieri, "Passive Geosynchronous SAR System Reusing Backscattered Digital Audio Broadcasting Signals," *TGARS*, vol. 36, no. 6, pp. 1973–1976, 1998.

[6] A. Monti-Guarnieri, M. Manzoni, D. Giudici, A. Recchia, and S. Tebaldini, "Vegetated Target Decorrelation in SAR and Interferometry: Models, Simulation, and Performance Evaluation," *Remote Sens.*, vol. 12, no. 16, p. 2545, Aug. 2020, doi: 10.3390/rs12162545.

[7] Y. Li, A. Monti Guarnieri, C. Hu, and F. Rocca, "Performance and requirements of GEO SAR systems in the presence of radio frequency interferences," *Remote Sens.*, vol. 10, no. 1, p. 82, 2018.

[8] A. Monti-Guarnieri *et al.*, "Passive sensing by Sentinel-1 SAR: Methods and applications," *Remote Sens. Environ.*, vol. 270, p. 112866, 2022.

[9] A. Monti-Guarnieri, D. Giudici, and A. Recchia, "Identification of C-Band Radio Frequency Interferences from Sentinel-1 Data," *Remote Sens.*, vol. 9, no. 11, p. 1183, Nov. 2017, doi: 10.3390/rs9111183.

[10] X. Dong, Y. Sui, Y. Li, Z. Chen, and C. Hu, "Modeling and Analysis of RFI Impacts on Imaging between Geosynchronous SAR and Low Earth Orbit SAR," *Remote Sens.*, vol. 14, no. 13, p. 3048, Jun. 2022, doi: 10.3390/rs14133048.

[11] A. R. Monteith and L. M. H. Ulander, "A Tower-Based Radar Study of Temporal Coherence of a Boreal Forest at P-, L-, and C-Bands and Linear Cross Polarization," *IEEE Trans. Geosci. Remote Sens.*, vol. 60, pp. 1–15, 2022, doi: 10.1109/TGRS.2021.3074098.

[12] J. B. Billingsley, *Low-Angle Radar Clutter Measurements and Empirical Models*. Norwich, NY, USA: William Andrew Publishing, 2002.

[13] J. R. Rodon, A. Broquetas, A. M. Guarnieri, and F. Rocca, "Geosynchronous SAR Focusing With Atmospheric Phase Screen Retrieval and Compensation," *IEEE Trans. Geosci. Remote Sens.*, vol. 51, no. 8, pp. 4397–4404, Agosto 2013, doi: 10.1109/TGRS.2013.2242202.

[14] J. Ruiz-Rodon, A. Broquetas, E. Makhoul, A. Monti Guarnieri, and F. Rocca, "Nearly Zero Inclination Geosynchronous SAR Mission Analysis With Long Integration Time for Earth Observation," *IEEE Trans. Geosci. Remote Sens.*, vol. 52, no. 10, pp. 6379–6391, 2014, doi: 10.1109/TGRS.2013.2296357.

[15] V. Queiroz de Almeida *et al.*, "Orbit. Performance and Observation Scenarios for Esa's Earth Explorer Mission Proposal Hydroterra," in *2021 IEEE International Geoscience and Remote Sensing Symposium IGARSS*, 2021, pp. 7740–7743. doi: 10.1109/IGARSS47720.2021.9554602.

[16] A. Ferretti, A. V. Monti-Guarnieri, C. M. Prati, F. Rocca, D. Massonnet, and others, *INSAR Principles B*. ESA publications, 2007.